Appl Microbiol Biotechnol (2015) 99:7369–7377
DOI 10.1007/s00253-015-6752-5

BIOENERGY AND BIOFUELS

Microbial lipid production by oleaginous *Rhodococci* cultured in lignocellulosic autohydrolysates

Zhen Wei[1,2] · Guangming Zeng[1,2] · Fang Huang[3] · Matyas Kosa[3] · Qining Sun[3] · Xianzhi Meng[3] · Danlian Huang[1,2] · Arthur J. Ragauskas[3,4]

Received: 2 April 2015 / Revised: 2 June 2015 / Accepted: 5 June 2015 / Published online: 4 July 2015
© Springer-Verlag Berlin Heidelberg 2015

Abstract Metabolic synthesis of single cell oils (SCOs) for biodiesel application by heterotrophic oleaginous microorganisms is being hampered by the high cost of culture media. This study investigated the possibility of using loblolly pine and sweetgum autohydrolysates as economic feedstocks for microbial lipid production by oleaginous *Rhodococcus opacus* (*R. opacus*) PD630 and DSM 1069. Results revealed that when the substrates were detoxified by the removal of inhibitors (such as HMF—hydroxymethyl-furfural), the two strains exhibited viable growth patterns after a short adaptation/lag phase. *R. opacus* PD630 accumulated as much as 28.6 % of its cell dry weight (CDW) in lipids while growing on detoxified sweetgum autohydrolysate (DSAH) that translates to 0.25 g/l lipid yield. The accumulation of SCOs reached the level of oleagenicity in DSM 1069 cells (28.3 % of CDW) as well, while being cultured on detoxified pine autohydrolysate (DPAH), with the maximum lipid yield of 0.31 g/l. The composition of the obtained microbial oils varied depending on the substrates provided. These results indicate that lignocellulosic autohydrolysates can be used as low-cost fermentation substrates for microbial lipid production by wild-type *R. opacus* species. Consequently, the variety of applications for aqueous liquors from lignocellulosic pretreatment has been expanded, allowing for the further optimization of the integrated biorefinery.

Keywords Autohydrolysis · Hardwood · Softwood · Fatty acid methyl ester · Oleaginous · *Rhodococcus* · Fermentation

✉ Guangming Zeng
zgming@hnu.edu.cn

✉ Arthur J. Ragauskas
aragausk@utk.edu

[1] College of Environmental Science and Engineering, Hunan University, Changsha 410082, People's Republic of China

[2] Key Laboratory of Environment Biology and Pollution Control, Hunan University, Ministry of Education, Changsha 410082, People's Republic of China

[3] School of Chemistry and Biochemistry, and Renewable Bioproducts Institute,, Georgia Institute of Technology,, 500 10th street N.W., Atlanta, GA 30332-0620, USA

[4] Department of Chemical and Biomolecular Engineering, Department of Forestry, Wildlife, and Fisheries, The University of Tennessee-Knoxville, 1512 Middle Drive, Knoxville, TN 37996-2200, USA

Introduction

With ever-increasing demand for renewable alternatives to conventional fuels, biodiesel, as an environment-friendly energy resource, has attracted considerable interest in recent years (Huang et al. 2010). Biodiesel is primarily obtained by the transesterification of triacylglycerols (TAGs) that make up plant oils (e.g., vegetable/seed oils) and animal fats, in the presence of a catalyst, yielding fatty acid methyl esters (FAMEs) (Du et al. 2004; Öner and Altun 2009; Ramadhas et al. 2005; Wyatt et al. 2005). To this date, this method is not fully optimized due to the high cost of raw materials that accounts for 60–75 % of operational expenses (Huang et al. 2010). To address this problem, a number of studies have focused on the development of low-cost and lipid-rich biological materials for biodiesel production. Recently, single cell oils (SCOs) from heterotrophic oleaginous microorganisms are considered as promising candidates given their short production cycle, high accumulation of lipids, and similar fatty acid composition to TAGs from vegetable oils (Kosa and Ragauskas 2011; Zhu et al. 2008). Some bacteria from the actinomycetes group, such as *Nocardia*, *Rhodococcus*, and

Mycobacterium, are capable of biosynthesizing and storing TAGs over 20 % of their own weight in lipids, a trait also known as oleaginicity (Kurosawa et al. 2010). *R. opacus* PD630, for instance, is able to accumulate substantial amounts of TAGs (80~90 % CDW) with gluconate as carbon source (Alvarez et al. 2000). However, metabolic synthesis of SCOs by heterotrophic oleaginous microorganisms is being hampered by the high cost of culture media (Gouda et al. 2008). To make microbial oils economically competitive, the utilization of cost-effective culture media from wastes or inexpensive renewable materials presents a great currently untapped potential.

Lignocellulose represents the largest and the most attractive biomass resources in the world (Fakas et al. 2009). On average, lignocellulosic biomass contains around 35–50 % of cellulose, 25–30 % of hemicellulose, and another 15–30 % of lignin. Hemicellulose is consisted of pentoses (xylose and arabinose) and hexoses (mannose, glucose, galactose, etc.), which are intimately associated with lignin to form a recalcitrant lignin-hemicellulose matrix that encrusts and protects cellulose in plant cell walls (Pu et al. 2013a). Therefore in biorefineries, pretreatments are needed as a first step to reduce the recalcitrance of this matrix, rendering the cellulose fibrils more accessible and amenable to further biological/chemical processing (Ayeni et al. 2013). Autohydrolysis, also called hydrothermal pretreatment, is considered to be a cost-effective and environment-friendly technology for the fractionation of lignocellulosic materials. During autohydrolysis pretreatment, lignocellulosic materials are treated with water as the fractionation reagent at elevated temperatures (160–240 °C) and the resulting liquid fraction is mainly composed of hemicellulose-derived sugars and oligomers, without causing significant dissolution of cellulose or lignin (Alvira et al. 2010; Romaní et al. 2011). The valorization of hemicellulosic sugars from these autohydrolysates to value-added products is crucial to economically enhance this type of biorefinery. Efforts in recent past have focused on the separation of the extracted hemicellulose to produce various types of polymers and chemicals such as organic acids (Abdel-Rahman et al. 2011). However, there are no reports concerning the utilization of lignocellulosic autohydrolysates directly as economic substrates for the production of microbial lipids that are composed of energy-rich TAGs.

The objective of this study is to evaluate the possibility of lignocellulosic autohydrolysates as sole carbon and energy sources for the growth and lipid accumulation of oleaginous *R. opacus* PD630 and DSM 1069. Loblolly pine and sweetgum were chosen as the starting materials for autohydrolysis because of their broad cultivation properties. Cell dry weight (CDW), lipid content (%CDW), lipid production, and the remaining concentration of monosaccharides in the substrates were monitored throughout all the experiments. In addition, the compositions of accumulated lipids at different stages were analyzed in detail.

Materials and methods

Starting biomass material

Loblolly pine (Pinus taeda *L*) and sweetgum (*Liquidambar styraciflua*) were collected from a University of Georgia research plot in Macon, GA. The stem wood material consisted of bark, xylem, and pith; It was debarked and chipped. Homogenized samples were used for all testing and analysis. All the biomass samples were stored at −5 °C during the course of this study. Prior to hot water pretreatment, these two biomasses were milled through a Wiley mill to pass 2-mm screen based on Tappi method T257 cm-02.

Hot water pretreatment

The loblolly pine and sweetgum sawdust were soaked overnight with deionized water, treated at 200 °C for 60 min with a solid-to-liquid ratio of 1:8. The extraction was carried out in a 1-l pressure reactor, with a Parr 4482 temperature controller (Parr Instrument Company, Moline, IL). The woodchips were soaked and treated in the reactor's glass liner. The initial pH of the extraction solution was approximately 6.5. After the pretreatment, the pH of the pine and sweetgum extraction solution was 4.5 and 4.0, respectively; the sample was filtered to separate the pretreated wood from the effluents. The effluent (PAH and SAH) was stored in a refrigerator before further characterization. The resulting solution was 1.23 and 1.08 % *w*/*v* solids in PAH and SAH, respectively.

Detoxification of PAH and SAH

The detoxification treatment includes overliming and adsorption. Firstly, the pH of the PAH and SAH was increased to 10.0 by addition of $Ca(OH)_2$. After 1 h, the hydrolysate was centrifuged and filtrated under vacuum and then acidified to pH 5.5 with 2 M H_2SO_4 for another 1 h. Centrifugation and filtration were conducted again to remove the precipitate and gypsum. Subsequently, 0.1 g/l Na_2SO_3 was added into the filtrate, followed by incubating the filtrate at 100 °C for 15 min. Then the overlimed autohydrolysate was recovered by vacuum filtration. For adsorption, Amberlite XAD-4 (Sigma-Aldrich, USA) was used. The resin was added to the overlimed autohydrolysate (1/5, *w*/*v*) and the mixture was incubated at 30 °C, 160 rpm overnight. Detoxified autohydrolysates (DPAH and DSAH) were obtained by filtration, then the pH was adjusted to 7.2 with 2 M NaOH or 2 M H_2SO_4 (Huang et al. 2009). The resulting solution was 0.35 and 0.25 % *w*/*v* solids in DPAH and DSAH, respectively.

Microorganisms, media preparation, precultivation, and cultivation

R. opacus PD630 (DSMZ 44193) and DSM 1069 strains were purchased from the German Collection of Microorganisms and Cell Cultures (DSMZ). Bacterial culture media, used here, were typical soy broth (TSB) and minimal media. The minimal media contained the following: 1.0 g $(NH_4)_2SO_4$, 1.0 g $MgSO_4 \cdot 7H_2O$, 0.015 g $CaCl_2 \cdot 2H_2O$, 1.0 ml trace element solution, 1.0 ml stock A solution, and 35.2 ml 1.0 M phosphate buffer. The trace element solution, stock A solution, and phosphate buffer were prepared as described by Chartrain et al. (1998). Bacteria were first incubated in TSB for 24 h then collected by centrifugation and washed several times with isotonic salt solution. Cells were then re-suspended and incubated in minimal media including PAH, SAH, DPAH, and DSAH separately. The original cells were seeded at a concentration of 5.4×10^4/ml optical density (OD ~0.1). All shake-flask fermentations were conducted under the same conditions of 30 °C and 150 rpm.

Analytical methods

Bacterial growth and lipid accumulation

After sampling, cells were pelletized by centrifugation and separated from the supernatants. Supernatants were stored for further characterization. Optical density (OD) was measured through UV absorbance at 600 nm when the cells were washed and re-suspended; subsequently, cells were washed by saline solution three times and freeze dried then measured as cell dry weights (CDW). All analyses were done in three replicates.

Lipid extraction and transesterification of freeze-dried cells (3~5 mg) were conducted as previously published (Wei et al. 2014). An Agilent 7890A GC system equipped with Agilent HP-5MS was used for measurements of FAMEs. Helium, 19.7 cm/s, was used as a carrier gas, and 2-μl samples were split injected (20:1); the temperature of the oven was set to 50 °C and kept for 5 min then was elevated by 15 °C/min until 325 °C and kept for 10 min. A 37-compound FAME mix from Sigma (CRM47885) was prepared in dichloromethane at 0.1, 0.25, and 0.5 mg/ml concentrations and was used as external standard. Accordingly, FAME contents were calculated in milligrams per milliliter, and these values are representative of approximate total lipid contents within cells, with a standard deviation ≤3.82 %. Unknown FAMEs were identified using Agilent's NIST08 library with above 95 % compound *m*/*z* spectrum similarity.

HMF and furfural analysis

The resulting 2-hydroxymethyl-furfural (HMF) and furfural content were measured using an Agilent 1200 HPLC system (Agilent Technologies, USA) equipped with a G2260A Agilent autosampler, a G2226A Agilent pump, a G1316A Agilent column, and a Refractive Index Detector (RID, G1362A) which was performed at 65 °C. Samples (50 μl) were filtered using a 0.45-μm PTFE syringe filter and eluted at 0.6 ml/min, with 0.01 M HNO_3 as the mobile phase. Standard mixture of HMF and furfural (0.4, 0.8, 1.2, 1.6, and 2 mg/ml) were used for the standard curve determination.

Substrate loss determination

Ammonium during the experiment was tested semi-quantitatively by EM Quant Ammonium Test from EMD Chemicals™, which shows 10, 30, 100, 300, and 500 mg/l ammonium ion contents. The mono-carbohydrates in the hydrolysates were quantified using a high-performance anion exchange chromatography with pulsed amperometric detection (HPAEC-PAD) using Dionex ICS-3000 (Dionex Crop., USA) (Davis 1998; Jung et al. 2010).

Results

Composition of PAH and SAH before and after detoxification

In addition to fermentable sugars, autohydrolysates derived from a lignocellulose material also contain inhibitors (such as HMF and furfural) that may negatively affect the growth of bacteria (Almeida et al. 2007). Although lipid-producing bacteria were reported to have the capability of tolerating the inhibition of these by-products (Wang et al. 2014), poor growth was observed when non-detoxified PAH and SAH were utilized as sole carbon sources (data not shown), suggesting that the presence of inhibiting compounds might have negative effects on the bacterial metabolism. In this study, a cost-effective method of overliming up to pH 10.0 with solid $Ca(OH)_2$ in combination with absorption by Amberlite XAD-4 was conducted to improve the autohydrolysates, by removing toxic sugar degradation products. All the chemicals used during the overliming treatment are economic, and this detoxification method has been widely used to remove contaminants from biomass hydrolysate (Chi et al. 2013; Palmqvist and Hahn-Hägerdal 2000a). Moreover, Amberlite absorbents have been reported to effectively remove the organic compounds and require low energy and, therefore, low costs for regeneration or renewal of absorbents (Frimmel et al. 1999). The changes of total reducing sugars, specific monosaccharide, and inhibitor components in PAH and SAH before and

after detoxification are summarized in Table 1. Under the current pretreatment conditions, PAH contained 2.33 g/l monosaccharides, which was approximately twice higher than those in SAH (1.01 g/l). These sugars primarily included galactose, glucose, xylose, and mannose, which accounted for 10, 48, 9, and 33 % in PAH and 4, 64, 19, and 13 % in SAH, respectively. Only a trace amount of arabinose was identified in both cases (data not shown).

With regard to inhibitors, high levels of HMF, primarily originated from the degradation of hexoses, were found in both the PAH (4.87 g/l) and SAH (2.04 g/l). In addition, a substantial amount of furfural (5.23 g/l) as dehydration product from pentose was identified in SAH due to high xylose content in hardwood, while the corresponding value in PAH was only 2.53 g/l. As shown in Table 1, HMF decreased 83 and 73 % in PAH and SAH, respectively, after detoxification. Furthermore, the concentrations of furfural in PAH and SAH also dropped by 94 and 87 %, respectively.

Bacterial growth and lipid production in DPAH and DSAH

Figure 1 shows the cell growth and lipid production of *R. opacus* PD630 and DSM 1069 cultured in DPAH and DSAH. After a short adaption phase (12–32 h), cells exhibited growth and lipid accumulation in the absence of inhibitors in all cases. In case of softwood autohydrolysates, both strains began to grow rapidly during the 12–32-h interval of incubation. After this phase, the growth rate decreased gradually and leveled off. The maximum CDW of PD630 and DSM 1069 appeared at 72 h, which were 0.96 and 1.03 g/l, respectively. However, when DSAH were used as sole carbon source, cell growth lagged about 24 h, especially for DSM 1069, which showed little growth until 32 h. However, the final CDW of PD630 and DSM 1069 cultured in DSAH reached 1.18 and 1.06 g/l.

It has been shown previously that *R. opacus* can accumulate lipid under nitrogen-deficient conditions (Kosa and Ragauskas 2012). As shown in Fig. 2, nitrogen decreased significantly during the first 8 h. After 56 h, nitrogen in all cases dropped to an undetectable level. It can be found that bacteria in DPAH consumed the nitrogen faster than those in DSAH.

The highest lipid content of PD630 in DPAH and DSAH appeared at 48 and 56 h, reaching 24.8 and 28.6 %, respectively (Fig. 1). For DSM 1069, oleaginicity was observed in DPAH, which was 28.3 % at 32 h. In all cases, lipid yield increased until reaching the maximum (32–56 h) and then fell, supporting further growth (Fig. 1). The maximum lipid yields in *R. opacus* PD630 (in DSAH) and DSM 1069 (in DPAH) reached 0.25 and 0.31 g/l, respectively. Table 2 compiles the maximum cell-specific and lipid-specific yields and volumetric productivities in the cells of PD630 and DSM 1069 with different carbon resource. It can be found that the maximum value of lipid volumetric productivities obtained in this study was 0.189 g/l day^{-1} that occurred in DPAH with DSM 1069.

Substrate loss during the fermentation

Figure 3 shows the changes of the selected reducing sugars' concentrations as well as the total sugar degradation rates during the course of the experiment, providing further understanding of carbon metabolism. It showed that hexose was preferentially consumed by bacterial cells in all cases compared to pentoses. During fermentation, glucose and galactose were preferably consumed. PD630 can use both glucose and

Table 1 Compositions of PAH and SAH after each step of detoxification treatment

Compound (g/l)	PAH (g/l)			SAH (g/l)		
	Original	Overliming	Adsorption	Original	Overliming	Adsorption
Galactose	0.23 ± 0.06 (1.63)	0.22 ± 0.04 (3.11)	0.20 ± 0.04 (5.76)	0.04 ± 0.003 (0.29)	0.03 ± 0.006 (0.33)	0.02 ± 0.007 (0.68)
Glucose	1.12 ± 0.12 (7.96)	1.11 ± 0.14 (15.67)	1.00 ± 0.03 (28.81)	0.65 ± 0.05 (4.72)	0.63 ± 0.05 (6.94)	0.59 ± 0.03 (20.17)
Xylose	0.22 ± 0.03 (1.88)	0.20 ± 0.05 (3.39)	0.17 ± 0.01 (5.88)	0.19 ± 0.04 (1.66)	0.16 ± 0.07 (2.12)	0.14 ± 0.01 (5.74)
Mannose	0.76 ± 0.08 (5.40)	0.71 ± 0.07 (10.02)	0.60 ± 0.05 (17.29)	0.13 ± 0.06 (0.94)	0.12 ± 0.04 (1.32)	0.11 ± 0.02 (3.76)
Total sugars	2.33 ± 0.13	2.24 ± 0.09	1.97 ± 0.12	1.01 ± 0.04	0.94 ± 0.10	0.86 ± 0.06
HMF	4.87 ± 0.15 (49.43)	2.22 ± 0.08 (44.78)	0.83 ± 0.02 (34.16)	2.04 ± 0.06 (21.17)	1.51 ± 0.10 (23.78)	0.56 ± 0.03 (27.35)
Furfural	2.53 ± 0.04 (33.70)	0.87 ± 0.08 (23.03)	0.15 ± 0.02 (8.10)	5.23 ± 0.18 (71.22)	3.17 ± 0.12 (65.51)	0.66 ± 0.09 (42.30)

The data in parentheses are mole percentages (%) of each component in dry weight of solids

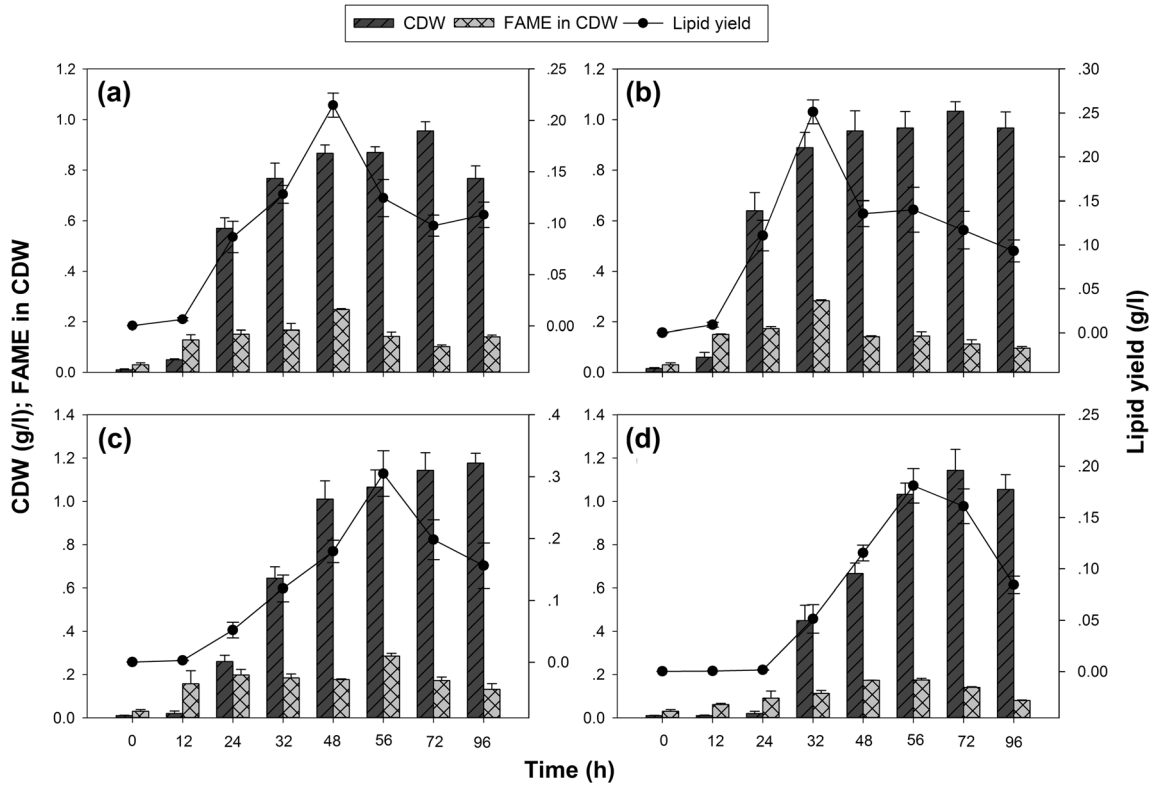

Fig. 1 Cell growth curves and lipid production of *R. opacus* PD630 and DSM 1069 in DPAH and DSAH. **a** DPAH with PD630, **b** DPAH with DSM 1069, **c** DSAH with PD630, and **d** DSAH with DSM 1069. Data are expressed as means of triplicate experiments and their standard deviations

galactose in parallel, which depleted completely during the initial 24 h. The utilization of these two types of sugars occurred alongside rapid growth as observed through CDW measurements. After consuming galactose and glucose, cells began to use mannose as carbon source and depleted it over the course of the fermentations. Regarding DSM 1069, a similar degradation profile of glucose and mannose was observed (Fig. 3b, d). Conversely, there was no obvious decrease in galactose concentration, indicating that DSM 1069 may not be able to digest galactose under the current experiment conditions. In addition, the minor xylose depletion during the whole timeframe suggested that *R. opacus* were not able to utilize xylose naturally. During the first 24 h, sugar consumption in DSAH was observed to be slower than that in DPAH, which was consistent with less cell growth demonstrated in Fig. 1. The total sugar degradation rates of DPAH and DSAH with PD630 were 95 and 85 %, while those with DSM 1069 were 91 and 90 %, respectively, indicating that most sugars in autohydrolysates can be utilized as carbon sources after detoxification.

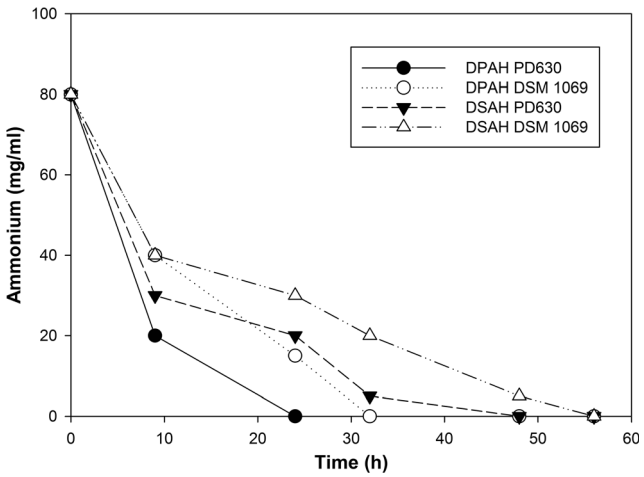

Fig. 2 Ammonium consumption in DSAH and DPAH with *R. opacus* PD630 and DSM 1069

Lipid composition analysis

Lipids derived from DPAH- and DSAH-grown cells were extracted and transmethylated simultaneously, followed by GC/MS analysis to investigate the specific fatty acid compositions. The fatty acid patterns at maximum lipid productivities are summarized in Table 3. Major fatty acids with chain lengths between 14 and 19 carbons were identified, while proportional differences of the lipid composition were depending on the provided carbon source. With DSAH as carbon source, both the strains can accumulate 26~29 % palmitic acid (C16:0) and 24~34 % stearic acid (C18:0),

Table 2 Maximum cell-specific and lipid-specific yields and volumetric productivities in the cells of PD630 and DSM 1069 with different carbon resources

Carbon source	Strain	T_{max} (h)	Y_{cell} (g/g)	T_{max} (h)	Y_{lipid} (g/g)	T_{max} (h)	dc_{lipid}/dt (g/l day)
DPAH	PD630	72	0.495 ± 0.02	48	0.111 ± 0.003	48	0.107 ± 0.003
	DSM 1069	72	0.581 ± 0.03	32	0.141 ± 0.002	32	0.189 ± 0.005
DSAH	PD630	96	1.458 ± 0.01	56	0.378 ± 0.009	56	0.131 ± 0.003
	DSM 1069	72	1.444 ± 0.04	56	0.228 ± 0.012	56	0.078 ± 0.001

The data in the table are shown as the mean values of measured results, and the standard deviations are from three replicates

which comprised the most abundant components. Conversely, not much stearic acid (C18:0) was observed in DPAH-grown bacteria, which accounted for only 14.5 and 10.3 % for PD630 and DSM 1069, respectively. Compared with cells in DSAH, both the strains cultured in DPAH accumulated more palmitoleic acid (C16:1) and oleic acid (C18:1), suggesting the environment in DPAH was beneficial to the storage of unsaturated acids. Furthermore, the accumulation of fatty acids with odd-numbered carbon chains was enhanced in bacterial cells with DPAH as carbon source. The impact of carbon source on fatty acid composition can be further demonstrated by comparing current results with the fatty acid pattern in *R. opacus* DSM 1069, utilizing pine organosolv pretreatment effluent (OPE) as carbon source (Wells et al. 2014) that resulted in significantly higher oleic acid (C18:1) accumulation (Table 3). In addition, only a minor amount of long chain fatty acids (<1.5 %), such as eicosanoic acid (C20:0), 11, 14-eicosadienoic acid (C20:2), heneicosanoic acid (C21:0), and docosanoic acid (C22:0) were also detected in all cases (data not shown).

Discussion

This study has demonstrated the potential to microbiologically convert lignocellulosic autohydrolysates into bio-oils by oleaginous *Rhodococci*. Loblolly pine and sweetgum were used as softwood and hardwood representatives and subjected to autohydrolysis with the same experimental parameters. As illustrated in Table 1, mannose in PAH was more abundant than in SAH, while the latter contained a higher proportion of xylose units. According to the chemical properties of softwood and hardwood, this result was in good agreement with previous literature (Palmqvist and Hahn-Hägerdal 2000b).

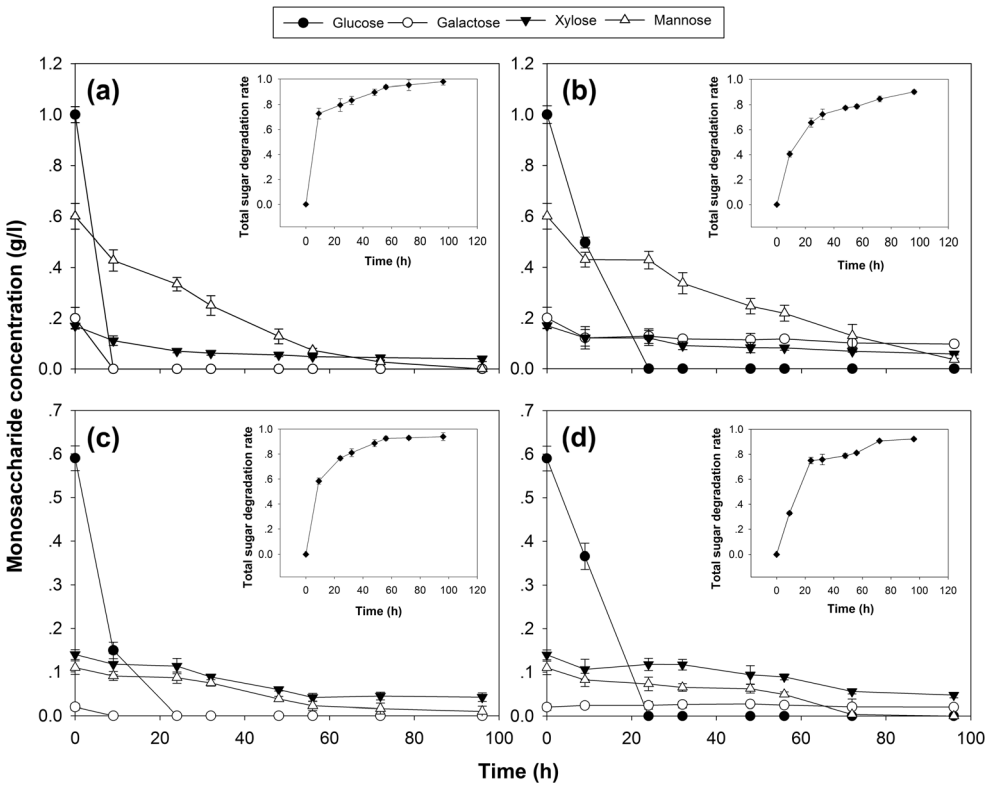

Fig. 3 Time course of sugar consumption when DPAH and DSAH were used as carbon source. **a** DPAH with PD630, **b** DPAH with DSM 1069, **c** DSAH with PD630, and **d** DSAH with DSM 1069. Illustrations of total sugar degradation rate are inserted in the corresponding graphs. Data are expressed as means of triplicate experiments and their standard deviations

Table 3 Fatty acid composition of the two cell lines in DPAH and DSAH at maximum lipid productivities

Strain	Carbon source	Fatty acids (%CDW)	SFA/UFA	*t* (h)	Relative proportion of fatty acid (*w*/*w*%)										
					C14:0	C15:0	C16:0	C16:1	C17:0	$^{10\text{-me}}$C16:0	C17:1	C18:0	$^{10\text{-me}}$C17:0	C18:1	C19:0
PD630	DPAH	24.8	2.1	48	2.3	7.0	26.7	13.9	2.7	2.5	4.4	14.5	2.8	11.4	4.8
	DSAH	28.6	5.4	56	2.9	2.9	28.7	7.8	1.6	2.2	2.0	34.0	1.4	4.8	5.7
DSM 1069	DPAH	28.3	2.0	32	2.7	6.8	25.4	14.6	3.5	2.5	7.5	10.3	3.8	9.4	6.8
	DSAH	17.5	3.8	56	3.0	3.6	26.6	10.1	2.4	4.0	2.2	24.2	1.8	7.1	7.3
	OPE	26.9	1.0	48	4.5	5	20	7.5	9	nd	7	17	nd	30	nd

The data in the table were shown as the mean values, and the standard deviation ≤3.82 %

nd not detected, *OPE* organosolv pretreatment effluent (Wells et al. 2014), *SFA* saturated fatty acids, *UFA* unsaturated fatty acids

However, in contrast to previous research (Pu et al. 2011, 2013b), glucose was observed to be dominant in both autohydrolysates, which was expected under high temperature conditions. HMF and furfural derived from sugar dehydration reactions detected herein (4.87 g/l HMF in PAH and 5.23 g/l furfural in SAH) reached the reported largest concentration in lignocellulosic hydrolysates (Almeida et al. 2009; Chen et al. 2009), causing the inhibition in microbial metabolism. After detoxification treatments, more than 73 % of HMF and furfural were effectively removed in both cases, which also increased the concentration of sugars in autohydrolysates that was believed to facilitate fermentation.

When DPAH and DSAH were used as sole carbon sources, both *R. opacus* DSM 1069 and PD630 exhibited cell viability, growth, and lipid accumulation with time. It is noteworthy that cells of the two strains cultured in DPAH went through a shorter lag phase and grew faster at the initial stage than those in DSAH, leading to the complete consumption of ammonium within 32 h (Figs. 1 and 2). This can be attributed to the higher concentration of total sugars in DPAH. Furthermore, the high proportion of xylose in DSAH can also limit the maximal cell growth because of its low digestibility by *R. opacus*. However, the adapted strains in DSAH began to grow rapidly with the final CDW even slightly higher than that on DPAH.

Both strains were observed to accumulate lipid at the level of oleaginicity (~28 *w*/*w*% CDW) during their growth. Even numbered monounsaturated and saturated fatty acids including palmitic acid (C16:0), stearic acid (C18:0), or/and oleic acid (C18:1) were in predominance, which implied the potential of such bacterial oils as biodiesel feedstocks (Li et al. 2008). Despite the similar lipid distribution between the samples, obvious proportional differences in specific fatty acids can be identified (Table 3). Using DPAH as carbon source contributed to the accumulation of unsaturated fatty acids (e.g., oleic acid) while DSAH growth cells tended to produce saturated fatty acids (e.g., stearic acid). The reason for this observation can be associated with the difference of carbon source and other residual substances between DPAH and DSAH. It has also been found in a previous study that the formation of oleic acid (C18:1) can be induced when OPE was used as carbon source (Wells et al. 2014). Furthermore, Gouda et al. (2008) confirmed the effects of diverse medium involving agro-industrial wastes on the variability of fatty acid patterns in *Gordonia* sp. DG. Therefore, it might be possible to select a certain carbon source for the production of an "engineered" lipid profile. Apart from carbon source types, the growth rate and changes in cultivation conditions such as, pH, temperature, and salinity can also impact the lipid production (Choi et al. 1982; Kosa and Ragauskas 2012; Li et al. 2008; Wei et al. 2014). Further research will focus on large-scale operation and optimization of high lipid yields and well-suited fatty acid composition for biodiesel applications.

To understand the carbon metabolism, HPAEC-PAD was used to analyze the substrate losses. The data (Fig. 3) revealed that hexoses are key carbon sources for the tested bacteria, and their utilizations have a sequence, such as glucose or/and galactose firstly, followed by the mannose as the alternative sugar. These results coincide with previous research, reporting that among the fermentable sugars in hydrolysates, glucose is considered as the desirable fermentation substrate for oleaginous microorganisms, while other hemicellulose-derived monosaccharides, such as mannose and galactose, can also be selectively utilized depending on the microbial species (Jin et al. 2015; Lee et al. 2011). Considering that xylose is the second most abundant sugar in hardwood, obtaining bacteria with xylose-degrading ability is of importance for better utilization of its hydrolysate. Recently, the xylose metabolic pathway has been successfully established in engineered strain of *R. opacus* PD630 (Xiong et al. 2012; Kurosawa et al. 2013).

Concisely, the current study demonstrated that oleaginous *R. opacus* PD630 and DSM 1069 can successfully use detoxified autohydrolysates of lignocellulosic biomass as sole carbon sources and accumulate lipid at oleaginous yields (~28 % *w*/*w* CDW). Additionally, the source of the feed material has a considerable effect on the fatty acid patterns in the growing

cells. Due to the wide availability of raw biomass in nature, lignocellulosic autohydrolysates can serve as economic microbial media. Furthermore, by carefully selecting the feed substrates, lipids with better properties for biodiesel applications can be obtained. Results shown here provide a sustainable route to reduce the lipid production costs as well as to improve the current biorefinery process.

Acknowledgments Z. Wei is grateful to the China Scholarship Council for awarding a scholarship under the State Scholarship Fund to pursue her study. This work will be used by Z. Wei for partial fulfillment of the degree requirement for her doctoral research at the College of Environmental Science and Engineering, Hunan University, Changsha, China. We also wish to acknowledge DOE (EE0006112) for their support via Synthetic Design of Microorganisms for Lignin Fuel, and Synthetic Design of Microorganisms for Lignin Fuel, the National Natural Science Foundation of China (51039001, 51378190) and the Program for Changjiang Scholars and Innovative Research Team in University (IRT-13R17).

Conflict of interest The authors declare that they have no competing interests.

References

Abdel-Rahman MA, Tashiro Y, Sonomoto K (2011) Lactic acid production from lignocellulose-derived sugars using lactic acid bacteria: overview and limits. J Biotechnol 156(4):286–301

Almeida JRM, Modig T, Petersson A, Hahn-Hagerdal B, Liden G, Gorwa-Grauslund M (2007) Increased tolerance and conversion of inhibitors in lignocellulosic hydrolysates by *Saccharomyces cerevisiae*. J Chem Technol Biotechnol 82(4):340–349

Almeida JRM, Bertilsson M, Gorwa-Grauslund MF, Gorsich S, Liden G (2009) Metabolic effects of furaldehydes and impacts on biotechnological processes. Appl Microbiol Biotechnol 82(4):625–638

Alvarez HM, Kalscheuer R, Steinbüchel A (2000) Accumulation and mobilization of storage lipids by *Rhodococcus opacus* PD630 and *Rhodococcus ruber* NCIMB 40126. Appl Microbiol Biotechnol 54(2):218–223

Alvira P, Tomás-Pejó E, Ballesteros M, Negro MJ (2010) Pretreatment technologies for an efficient bioethanol production process based on enzymatic hydrolysis: a review. Bioresour Technol 101(13):4851–4861

Ayeni AO, Hymore FK, Mudliar SN, Deshmukh SC, Satpute DB, Omoleye JA, Pandey RA (2013) Hydrogen peroxide and lime based oxidative pretreatment of wood waste to enhance enzymatic hydrolysis for a biorefinery: process parameters optimization using response surface methodology. Fuel 106:187–194

Chartrain M, Jackey B, Taylor C, Sandford V, Gbewonyo K, Lister L, Dimichele L, Hirsch C, Heimbuch B, Maxwell C, Pascoe D, Buckland B, Greasham R (1998) Bioconversion of indene to *cis* (1S,2R) indandiol and *trans* (1R,2R) indandiol by *Rhodococcus* species. J Ferment Bioeng 86(6):550–558

Chen X, Li Z, Zhang X, Hu F, Ryu DDY, Bao J (2009) Screening of oleaginous yeast strains tolerant to lignocellulose degradation compounds. Appl Biochem Biotechnol 159(3):591–604

Chi ZY, Rover M, Jun E, Deaton M, Johnston P, Brown RC, Wen ZY, Jarboe LR (2013) Overliming detoxification of pyrolytic sugar syrup for direct fermentation of levoglucosan to ethanol. Bioresour Technol 150:220–227

Choi SY, Ryu DDY, Rhee JS (1982) Production of microbial lipid: effects of growth rate and oxygen on lipid synthesis and fatty acid composition of *Rhodotorula gracilis*. Biotechnol Bioenerg 24(5):1165–1172

Davis MW (1998) A rapid modified method for compositional carbohydrate analysis of lignocellulosics by high pH anion-exchange chromatography with pulsed amperometric detection (HPAEC/PAD). Wood Chem Technol 18(2):235–252

Du W, Xu YY, Zeng J, Liu DH (2004) Novozym 435-catalysed transesterification of crude soya bean oils for biodiesel production in a solvent-free medium. Biotechnol Appl Biochem 40(2):187–190

Fakas S, Papanikolaou S, Batsos A, Galiotou-Panayotou M, Mallouchos A, Aggelis G (2009) Evaluating renewable carbon sources as substrates for single cell oil production by *Cunninghamella echinulate* and *Mortierella isabellina*. Biomass Bioenerg 33(4):573–580

Frimmel FH, Assenmacher M, Sörensen M, Abbt-Braun G, Gräbe G (1999) Removal of hydrophilic pollutants from water with organic adsorption polymers: part I. Adsorption behaviour of selected model compounds. Chem Eng Process 38(4–6):601–609

Gouda MK, Omar SH, Aouad LM (2008) Single cell oil production by *Gordonia* sp DG using agro-industrial wastes. World J Microbiol Biotechnol 24(9):1703–1711

Huang C, Zong MH, Wu H, Liu QP (2009) Microbial oil production from rice straw hydrolysate by *Trichosporon fermentans*. Bioresour Technol 100(19):4535–4538

Huang GH, Chen F, Wei D, Zhang XW, Chen G (2010) Biodiesel production by microalgal biotechnology. Appl Energy 87(1):38–46

Jin MJ, Slininger PJ, Dien BS, Waghmode S, Moser BR, Orjuela A, da Costa SL, Balan V (2015) Microbial lipid-based lignocellulosic biorefinery: feasibility and challenges. Trends Biotechnol 33(1):43–54

Jung S, Foston M, Sullards MC, Ragauskas AJ (2010) Surface characterization of dilute acid pretreated *Populus deltoides* by ToF-SIMS. Energ Fuel 24:1347–1357

Kosa M, Ragauskas AJ (2011) Lipids from heterotrophic microbes: advances in metabolism research. Trends Biotechnol 29(2):53–61

Kosa M, Ragauskas AJ (2012) Bioconversion of lignin model compounds with oleaginous *Rhodococci*. Appl Microbiol Biotechnol 93(2):891–900

Kurosawa K, Boccazzi P, de Almeida NM, Sinskey AJ (2010) High-cell-density batch fermentation of *Rhodococcus opacus* PD630 using a high glucose concentration for triacylglycerol production. J Biotechnol 147(3–4):212–218

Kurosawa K, Wewetzer SJ, Sinskey AJ (2013) Engineering xylose metabolism in triacylglycerol producing *Rhodococcus opacus* for lignocellulosic fuel production. Biotechnol Biofuel 6:134

Lee KS, Hong ME, Jung SC, Ha SJ, Yu BJ, Koo HM, Park SM, Seo JH, Kweon DH, Park JC, Jin YS (2011) Improved galactose fermentation of *Saccharomyces cerevisiae* through inverse metabolic engineering. Biotechnol Bioeng 108(3):621–631

Li Q, Du W, Liu DH (2008) Perspectives of microbial oils for biodiesel production. Appl Microbiol Biotechnol 80(5):749–756

Öner C, Altun S (2009) Biodiesel production from inedible animal tallow and an experimental investigation of its use as alternative fuel in a direct injection diesel engine. Appl Energy 86(10):2114–2120

Palmqvist E, Hahn-Hägerdal B (2000a) Fermentation of lignocellulosic hydrolysates. I: inhibition and detoxification. Bioresour Technol 74(1):17–24

Palmqvist E, Hahn-Hägerdal B (2000b) Fermentation of lignocellulosic hydrolysates. II: inhibitors and mechanisms of inhibition. Bioresour Technol 74(1):25–33

Pu Y, Treasure T, Gonzalez RW, Venditti R, Jameel H (2011) Autohydrolysis pretreatment of mixed hardwood to extract value prior to combustion. Bioresources 6(4):4856–4870

Pu Y, Hu F, Huang F, Davison BH, Ragauskas AJ (2013a) Assessing the molecular structure basis for biomass recalcitrance during dilute acid and hydrothermal pretreatments. Biotechnol Biofuel 6:15

Pu Y, Treasure T, Gonzalez R, Venditti RA, Jameel H (2013b) Autohydrolysis pretreatment of mixed softwood to produce value prior to combustion. Bioenerg Res 6(3):1094–1110

Ramadhas AS, Jayaraj S, Muraleedharan C (2005) Biodiesel production from high FFA rubber seed oil. Fuel 84(4):335–340

Romaní A, Garrote G, López F, Parajó JC (2011) *Eucalyptus globulus* wood fractionation by autohydrolysis and organosolv delignification. Bioresour Technol 102(10):5896–5904

Wang B, Rezenom YH, Cho KC, Tran JL, Lee DG, Russell DH, Gill JJ, Young R, Chu KH (2014) Cultivation of lipid-producing bacteria with lignocellulosic biomass: effects of inhibitory compounds of lignocellulosic hydrolysates. Bioresour Technol 161:162–170

Wei Z, Zeng GM, Kosa M, Huang DL, Ragauskas AJ (2014) Pyrolysis oil-based lipid production as biodiesel feedstock by *Rhodococcus opacus*. Appl Biochem Biotechnol 175(2):1234–1246

Wells Jr T, Wei Z, Ragauskas AJ (2014) Bioconversion of lignocellulosic pretreatment effluent via oleaginous *Rhodococcus opacus* DSM 1069. Biomass Bioenerg 72:200–205

Wyatt VT, Hess MA, Dunn RO, Foglia TA, Haas MJ, Marmer WN (2005) Fuel properties and nitrogen oxide emission levels of biodiesel produced from animal fats. Am Oil Chem Soc 82(8):585–591

Xiong XC, Wang X, Chen SL (2012) Engineering of a xylose metabolic pathway in *Rhodococcus* strains. Appl Environ Microbiol 78(16): 5483–5491

Zhu LY, Zong MH, Wu H (2008) Efficient lipid production with *Trichosporon fermentans* and its use for biodiesel preparation. Bioresour Technol 99(16):7881–7885